Real-time Tracking of Stress Propagation using Distributed Granger Causality

Eun Kyung Lee, Parul Pandey, and Dario Pompili
NSF Center for Cloud and Autonomic Computing
Department of Electrical and Computer Engineering, Rutgers University, New Brunswick, NJ
e-mail: {eunkyung_lee, parul_pandey, pompili}@cac.rutgers.edu

ABSTRACT

Stress is one of the key factors that impacts the quality of our daily life. It is known that stress can propagate from one individual to others working in close proximity or towards a common goal, e.g., in a military operation or workforce, thus affecting productivity, efficiency, and the ability to make rational decisions. Real-time assessment of the stress of individuals alone is, however, not sufficient as understanding its *source* and *direction* in which it propagates in a group is equally if not more important. In this paper, the direction of propagation and magnitude of influence of stress in a group of individuals are studied by applying real-time, in-situ analysis of *Granger Causality*. G-causality has established itself as one of the promising non-invasive approaches in operational neuroscience to reveal the direction of influence between brain areas by analyzing temporal precedence. Extending G-causality analysis on real-time group data faces, however, communication and computation challenges, to address which a distributed mobile computational framework is employed and workflows defining how data and tasks are divided among the entities of the framework are designed.

1. INTRODUCTION

Motivation: Stress is one of the key factors affecting physical and mental wellbeing, which are essential in any environment where high level of performance is required and sought. Research has shown that doctors and army personnel experience high level of stress as tolerance for errors in their profession is very low. High stress can significantly impair the ability to perform tasks and make rational decisions, which may impact a patient's life in case of doctors and national security in case of army personnel [12]. In [16], physicians have reported that medical errors in which they had been involved increased their anxiety about the potential for future errors and negatively affected their confidence in their abilities as physicians. It is well documented that high level of stress experienced by doctors can lead to physical, psychological, and emotional harm, in particular, burnout [3]. Stress can also *propagate* from one individual to others working in close proximity or towards a common goal, e.g., in a military operation or workforce. The members in the team can be affected by *anxiogenic behavior*, i.e., a behavior that induces anxiety and stress, of any/few members of the team. We term the stress experienced by individuals in a group as *group stress*.

Vision: Stress detection can provide us information of the state of mind of an individual and can help enhance his/her current productivity. Two physiological signals are required for real-time stress detection, namely, *Galvanic Skin Response (GSR)* and *Heart Rate (HR)*, as both provide accurate and precise information on the physiological situations of the individuals [5]. The rapid growth of non-invasive sensing and low-power wireless communication technologies has enabled continuous physiological signal acquisition using compact wearable biomedical sensor nodes. However, quantifying stress of an individual is not sufficient as the ultimate goal is to understand the *source of stress* in a group and the *direction* in which it propagates to the members. The real-time group-stress detection allows us to make decisions based on the mental state of individuals for a latency-critical application. As an example, consider that a team has to be formed for a strategic military mission; in this case, real-time group-stress detection can give us insights into the current state of mind of different army men. The army men who can perform tasks without being overwhelmed by those at higher ranks, or by anxiogenic behavior of other team members, should be selected. This will empower army personnel who are in better condition (less stressed) by putting them in charge of the situation; also, it will help improve productivity and reorganize hierarchy beyond existing ranks and roles. Hence, our interest is in understanding the real-time *direction* and *magnitude* (i.e., extent) of influence of stress from one person to another in the same group.

Tool to study propagation of stress: In neuroscience, Granger Causality (or G-causality) has established itself as one of the promising *non-invasive* approaches to reveal the direction of influence between brain areas by analyzing temporal precedence: if a signal change in area A consistently precedes a signal change in area B, then A is said to Granger-cause B [9]. G-causality has been successfully used in many domains, e.g., for characterizing causal connectivity patterns across different conscious levels (e.g., sleep anesthesia, normal wakefulness) [2]. While G-causality has been used in literature to analyze causal temporal precedence between signals of an individual, in this work we extend such ap-

proach and advocate the use of this tool to study causality between physiological signals from two different individuals. We focus on detection of stress of individuals in a team and establish the magnitude of influence of stress and its direction of propagation in a group by applying real-time, in-situ G-causality analysis. Note that G-causality provides a much stringent condition on causation than just observing high correlation with some lag-lead relationship. In our paper, we measure both correlation and causality in group-stress data, study their relationship in different scenarios for different time lags, and establish where correlation between stress data of different individuals is significantly higher than causality and viceversa.

Challenges: Real-time G-causality analysis of group-stress data faces communication and computation challenges. Firstly, large amount of data has to be moved among the sensor nodes, which are attached to members of the group (*communication bottleneck*). Secondly, group G-causality analysis requires solving multiple linear regression problems (*computation bottleneck*); the computation complexity of such pairwise analysis increases quadratically with the number of people in the group. To address these challenges, we propose to execute G-causality workflows in a distributed manner. We refer to our earlier work on distributed mobile computing grid [15] to enable distributed G-causality. The distributed grid is divided into two major entities, namely, 1) *middleware*, which solves the communication bottleneck by moving the data within the network efficiently, and 2) *framework*, which takes care of the high computation aspect of the problem by assigning computation tasks "optimally" to the different entities of the distributed grid (computation nodes). In this work, we also present workflows, which define the tasks as well as their input/output relationship, that can be executed by the different entities of the distributed framework to overcome the above challenges.

There are a few challenges to overcome in order to enable G-causality. Firstly, G-causality requires the data to be *covariance stationary* [11], which is a requirement that is not always possible to meet. Significant individual-specific preprocessing steps need to be applied in order to make the data stationary (e.g., testing subsets of data to determine the length over which the data is stationary). In order to estimate G-causality, it is required to determine the *time lag* between the two signals under investigation; a minimum and maximum time lag should be specified, and within such range an optimal lag should be determined on the fly. The complexity of this computational task increases as the measure of this range, i.e., the difference between the max and min lag, increases. Figure 1 envisions two scenarios, a civilian (left) and a military (right), where sensors on the body of medical personnel and soldiers, respectively, are used to continuously collect various vital signs and nearby rugged computing devices organized by our mobile computing framework are used for compute-intensive group-stress analysis.

Our Contribution: The major contributions of this paper include: 1) enabling compute-intensive group Granger-causality analysis of stress using our mobile-grid framework; 2) studying the direction of propagation and magnitude of stress from one member of the group to the other(s); 3) designing workflows on how data and tasks are divided among

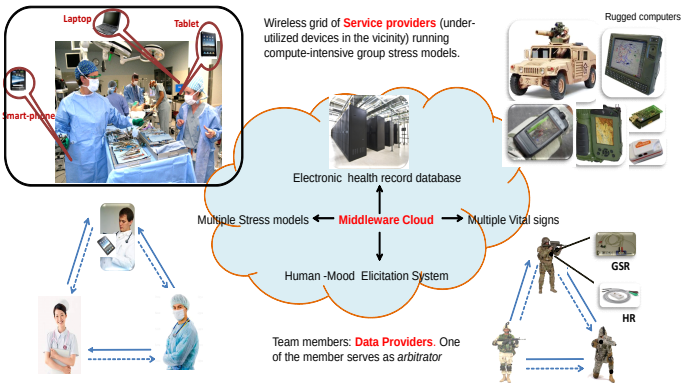

Figure 1: Role-based resource provisioning framework for real-time tracking of stress propagation.

the different entities of the framework. The rest of the paper is organized as follows: in Sect. 2, we present our proposed solution to enable distributed G-causality; in Sect. 3, we describe our experimental methodology and results; finally, in Sect. 4, we present our conclusions and plans for future work.

2. PROPOSED SOLUTION

Our group-stress analysis aims at analyzing in real time *direction of propagation* and *magnitude* of stress between different members of a group. Such a real-time analysis poses, however, several communication (data exchange among sensors) and computation challenges (multiple linear regression problem). To overcome these challenges, we propose solving G-causality in a distributed way via our mobile computing framework. In this section, we briefly give an overview of the theory of G-causality; then, we discuss the workflow (sequence of tasks) for the distributed execution of G-causality. We also introduce the entities of our distributed framework and explain how such entities collaborate to perform different tasks of the workflow.

Distributed Granger Causality: A time series $\mathbf{x} = \{x_1, x_2, \ldots, x_t, \ldots\}$ is said to Granger-cause another time series $\mathbf{y}$ if including information about the past of $\mathbf{x}$ significantly increases the prediction accuracy of the current value y_t of $\mathbf{y}$ in comparison to predicting it based *only* on the past values of y alone. Granger Causality was initially introduced in [6], where the authors implemented it using two vector Auto-Regressive (AR) models; the first, called *restricted model*,

$$x_t = \sum_{j=1}^{P} a_j x_{t-j} + \delta_{1t}, \quad y_t = \sum_{j=1}^{P} a_j y_{t-j} + \gamma_{1t}, \qquad (1)$$

calculates how much two time series, $\mathbf{x}$ and $\mathbf{y}$, can be 'explained' by their own past ($x_{t\text{-}j}$ and $y_{t\text{-}j}$, with $j = 1, 2, \ldots$), resulting in residual error variances $\Delta_1 = var(\delta_{1t})$ and $\Gamma_1 = var(\gamma_{1t})$ (the model order is represented by P, which specifies how many previous time points are taken into account, and the length of the time series by T, with $P < T$).

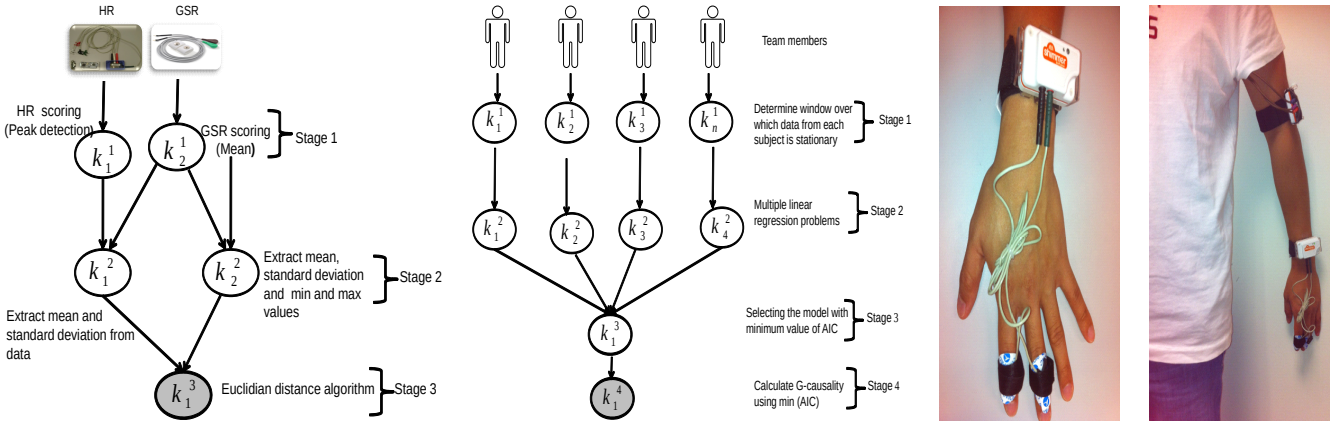

Figure 2: (a) Workflow designed to determine stress of an individual from his/her vital signs; (b) Workflow designed to execute G-causality in our distributed computing framework (*note that the output of the stress workflow serves as input to the G-causality workflow*); Experimental setup to measure (c) skin response using Galvanic Skin Response (GSR) sensors and (d) heart rate using Electrocardiogram (ECG) sensors.

In the second, called *unrestricted model*,

$$x_t = \sum_{j=1}^{P} a_j x_{t-j} + \sum_{j=1}^{P} b_j y_{t-j} + \delta_{2t},$$
$$y_t = \sum_{j=1}^{P} a_j y_{i-j} + \sum_{j=1}^{P} b_j x_{t-j} + \gamma_{2t}, \quad (2)$$

the prediction is based on the time series' own past and the past of the other time series. This results in residual error variances $\Delta_2 = var(\delta_{2t})$ and $\Gamma_2 = var(\gamma_{2t})$. The linear influence from $\mathbf{x}$ to $\mathbf{y}$, $\mathcal{F}_{\mathbf{x}\to\mathbf{y}}$, and from $\mathbf{y}$ to $\mathbf{x}$, $\mathcal{F}_{\mathbf{y}\to\mathbf{x}}$, can now be calculated as the ratio between the variances of the residual error, i.e.,

$$\mathcal{F}_{\mathbf{x}\to\mathbf{y}} = \ln \frac{var(\gamma_{1t})}{var(\gamma_{2t})} = \ln \frac{\Gamma_1}{\Gamma_2}, \; \mathcal{F}_{\mathbf{y}\to\mathbf{x}} = \ln \frac{var(\delta_{1t})}{var(\delta_{2t})} = \ln \frac{\Delta_1}{\Delta_2}. \quad (3)$$

A reduction in error variance when including the past of another time series results in a larger $\mathcal{F}$-ratio. The difference G-causality, i.e., $\mathcal{F}_{\mathbf{x}\to\mathbf{y}} - \mathcal{F}_{\mathbf{y}\to\mathbf{x}}$, was calculated to assess the dominant direction of information flow.

Selection of Time Lag: Selecting the time lag is an important problem in G-Causality. The estimation of AR models requires as a parameter the number of time-lags P to include, i.e., the model order. Too few lags can lead to a poor representation of the data, whereas too many of them can lead to problems in the model estimation [11]. Two criteria have been introduced in the literature, namely the Akaike Information Criterion (AIC) [1] and the Bayesian Information Criterion (BIC) [10] to estimate the model order. For n variables we have,

$$AIC(P) = \ln(|\mathbf{\Sigma_2}|) + \frac{2Pn^2}{T},$$
$$BIC(P) = \ln(|\mathbf{\Sigma_2}|) + \frac{\ln(T)Pn^2}{T}. \quad (4)$$

where $\mathbf{\Sigma_2}$ is the noise covariance matrix of the unrestricted model and $|\cdot|$ indicates the determinant of a matrix. AIC is calculated for a set of model orders and the order which gives the minimum value of AIC is selected as the model order of the AR model to determine G-causality between two time series.

Designing Workflow for G-causality: To enable the distributed G-causality, we design a workflow that indicates the different tasks that have to be executed in parallel and the sequential steps that have to be taken to determine G-causality. A workflow is composed of multiple *stages* with a set of tasks $\mathcal{K}^i = \{k_j^i\}, j = 1, \ldots, |\mathcal{K}^i|$, to be performed at each stage i. Let M be the total number of stages, i.e., $i = 0, \ldots, M-1$. Figure 2(a) depicts the workflow for stress detection and stress-level rating [13, 4], which uses vital-sign data acquired from biomedical as well as kinematic sensors. Stage 1 of this workflow is purely composed of data-analysis tasks, whereas Stages 2 and 3 are composed of data-manipulation or decision-making tasks. In Stage 1, Heart Rate (HR) and GSR are each given a score $[0, 1]$ (0 corresponds to low, 1 to high) based on simple manipulations of the corresponding sensor outputs. The assignment of these normalized scores requires domain knowledge and is in some cases subject specific (as in GSR and HR). In the second stage, we determine the mean, standard deviation, and minimum and maximum value of GSR and HR from the data. In the last stage, we use our Euclidian distance algorithm (explained later) to determine the overall stress.

Figure 2(b) shows the workflow diagram to compute G-causality. The G-causality workflow takes as input the output of the stress workflow model, which is the stress experienced by each member of the team measured over a period of time. In the first stage of the G-causality workflow, each sensor node performs pre-processing steps and checks the stationarity of the stress data [6]. In the case the data is not stationary, the sensor nodes determine the time window over which the data is stationary. In the second stage, each sensor node solves multiple linear regression problems, which determine the model order. Each node also receives data from all the other sensor nodes in the group and calculates the model order from each pair of nodes. As the last stage,

each node determines the G-causality for each pair of group members.

Note that the computation complexity to determine the stress for a team increases *linearly* with the number of team members. On the other hand, the computation complexity to determine the magnitude of G-causality for a team increases *quadratically* with the number of team members. This is because we estimate G-causality pair-wise, i.e, we calculate G-causality between every two members of the team. To determine G-causality between any pair of team members, the compute intensive task is the estimation of time lag, which requires solving a linear regression problem. The dominant operation in a linear regression problem is matrix inversion, which requires $N^3 + N^2 + N$ floating point operations (flops), where N is the length of the stress data of an individual.

Distributed Computing Framework: To solve the challenges faced by a real-time implementation of G-causality, we propose to compute G-causality using our distributed computing framework [15]. The entities of the distributed computing grid may at any time play one or more of the following three logical roles: i) *service requester,* which places requests for workloads that require additional data and/or computing resources from other devices, ii) *service provider,* which can be a data provider, resource provider, or both, and iii) a *broker* (usually, the base station), which processes the requests from the requesters, determines the set of service providers that will provide or process data, and distributes the workload tasks among them. The service requester offloads (shares) the task of executing compute-intensive algorithms to (with) the service providers by submitting service requests to one of the brokers. Resource providers lend their computational (CPU cycles), storage (volatile and non-volatile memory), and communication (i.e., network interface capacity) resources for processing data. The broker is aided by an energy-aware resource allocation engine that distributes the workload tasks optimally among the service providers. Our framework applies to applications exhibiting data parallelism as well as to applications exhibiting task parallelism. The broker is made aware of the availability of service providers through voluntary service advertisements from the service providers.

Entities involved in our experimental setup: In our experimental setup all the sensor nodes attached to group members serve as data providers and service providers. All the devices in the vicinity, i.e., that are one-hop distance away from the sensor nodes, also serve as service provider. They provide their computational power for group-stress analysis. We assume that the nodes communicate with the devices in the vicinity over a piconet. The nodes collect data for a pre-defined interval of time and later broadcast the data sequentially with a pre-defined guard band to the nearby devices forming the distributed computing grid. The division of tasks among devices is based on the workflow described earlier. From our workflow (Fig. 2), we can see that Stage 0 is composed entirely of data-collection tasks, which can be performed only at the data providers (sensor nodes). The computation and final tasks (at any stage $i \geq 1$), however, can be performed at any service provider (sensors on body or other nearby computing devices).

Cloud-assisted Stress Analysis: A Cloud is a trusted, resource-rich cluster of computers that is well-connected to the Internet. Clouds have higher computing power than that available to an elastic pool of resources (services providers) in the field. Hence, this gives us an opportunity for more thorough analysis of the collected stress data. On the other hand, local computing grid is used for time-critical group-stress analyses, e.g., to select team members for a strategic military operation. In this paper, we have focused on two physiological signals; however, several other physiological signals, e.g., skin temperature, breath, blood pressure volume, and pupil dilation, have also been used in the literature for stress detection. Cloud computing gives us an opportunity to use an ensemble of physiological signals and stress models to obtain a better estimate of stress. In fact, multiple physiological signals can help design human emotions elicitation system and responses to them by using supervised learning algorithms [8].

Also, Clouds can serve as a database by storing stress history of multiple people over a period of time. Every time stress is determined by a local distributed grid, it can be sent to the Cloud. This way, the latest stress data of a person can be compared with stored stress data so to monitor the evolution of the stress of the person over time and over activities, given a certain context. The Cloud can thus tabulate and send to a group leader (supervisor of a group whose group stress is being analyzed) the tasks in which a person is more productive and the group of people with whom a person works more productively. A ranking algorithm can be used to process this information.

3. PERFORMANCE EVALUATION

We provide here details about our testbed and the experiment methodology; then, we present experiment scenarios and discuss the results. Specifically, we present how stress can be quantified real time from physiological signals as well as how it propagates from one group member to another (in terms of magnitude and direction).

Experimental Setup: To measure GSR and HR, we have used non-invasive GSR and ECG sensors; the former measures the change in electro-dermal activity (increase in conductance) as sweat glands are stimulated for a hydrate solution, while the latter measures the heart rate of an individual. Both sensors are part of our mobile framework via Bluetooth connections and stream GSR and ECG measurements. The data stream collected on-line feeds our framework, and hence, our group-stress analysis application. Figure 2(c) and (d) show the placement of the sensors on the body. The sampling rate of GSR and ECG sensors are set to 51.2 Hz; we have employed wavelet transformation [7] to calculate HR based on the peak-to-peak distance extracted from the ECG measure. We give these measurements as an input to the stress model in Fig. 2(a) to determine stress.

Quantification of Stress: Our model quantifies the level of stress based on GSR and HR measurements. The level of stress, which ranges in $[0 - 1]$, is used as input parameter for the G-causality calculation. In general, GSR and HR show increase in value with increase in stress but, as different group members react differently even for the same type and degree of stress, it is hard to quantify the level of the stress

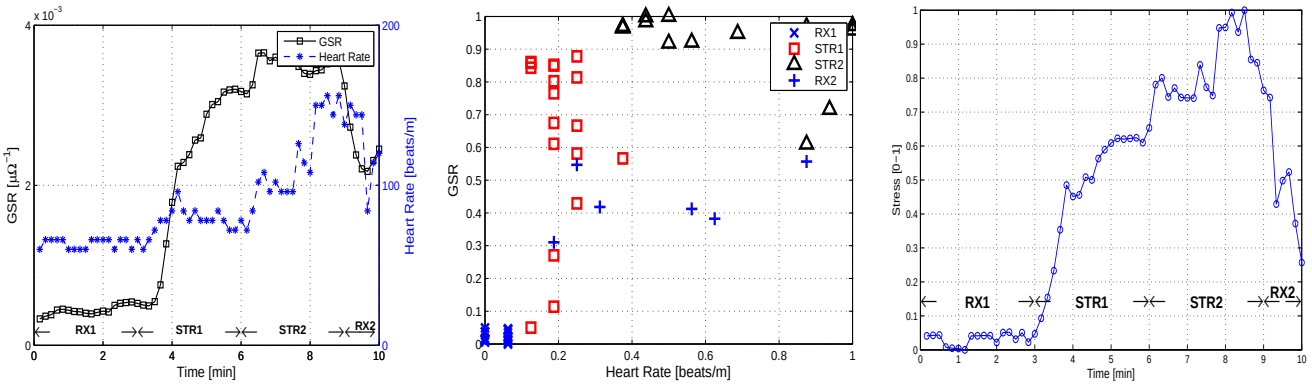

(a) (b) (c)

Figure 3: (a) Raw GSR and HR measurements under four different phases (RX1 and RX2 indicate relaxed phase, while STR1 and STR2 represent mental- and physical-stress phase, respectively); (b) Normalized GSR-HR data; (c) Stress calculated via the stress model in Fig. 2(a), which uses GSR and HR as inputs.

across group members. Hence, we profile each individual based on different level of stress phases and extract the features from the measurement. Our profiling phase extracts the statistical features of sensor values and normalizes them to make the stress level comparable to that of other group members. Specifically, we have considered the measurement of HR and GSR as stochastic signals, and extracted the features (i.e., mean μ, standard deviation σ, maximum max, and minimum min) of HR and GSR signal in different test stress phases (e.g., relaxed and under-stressed phases).

Figure 3(a) plots raw GSR and HR signals during our experiment and shows that the measurements depend on the stress level induced by our experiments. The experiments are composed of four phases: two relaxed phases (RX1 and RX2) and two under-stress phases (STR1 and STR2). RX1 indicates the relaxed phase before the experiment starts while RX2 indicates the relaxed phase at the end; STR1 indicates a phase where a group member is under stimulating task (hyperventilation) and STR2 indicates a phase where a group member is under a physical exercise. From our experiments, we have observed that physical stress significantly changes HR rather than GSR, whereas mental stress (anxiety reflected in hyperventilation) significantly changes GSR rather than HR. Therefore, by collecting simultaneously HR and GSR signals, we can study both the mental and physical stress experienced by an individual. To quantify the propagation of mental stress, we focused on calculating stress from GSR signals. We denote as h_r^m and g_r^m to indicate the raw HR and the GSR signals of a group member r under stress phase m, where R is the number of group members and M is the number of stress phase. After acquiring the raw data from the sensors, we normalize the collected measurement g_r^m and h_r^m, $\forall\ r = \{1, 2, \ldots, R\}$ and $m = \{1, 2, \ldots, M\}$. First, we extract the minimum and maximum value of $g_r^{min} = \min(g_r^1, g_r^2 \ldots g_r^M)$ and $g_r^{max} = \max(g_r^1, g_r^2 \ldots g_r^M)$, and the same for h_r^{min} and h_r^{max} among the different R phases. We normalize g_r and h_r as,

$$g_r^{norm} = \frac{g_r - g_r^{min}}{g_r^{max} - g_r^{min}}, \quad h_r^{norm} = \frac{h_r - h_r^{min}}{h_r^{max} - h_r^{min}}. \qquad (5)$$

Figure 3(b) shows normalized [0-1] HR-GSR data in a 2D plain. We calculate the Euclidian distance of each measurement in the GSR-HR plain to compute the stress level and normalize it to obtain the final stress level, which ranges in [0-1] as shown in Fig. 3(c).

Distributed Computation of G-causality: We compared the performance of centralized execution of G-causality against its distributed computation using our mobile computing framework. The metric for comparison is *time taken* to execute G-causality for a team of people. We compared the centralized execution (where data is given from all nodes to a sink node for computation) (Schedule-1) with Round-Robin (in which we distribute an equal number of tasks to all nodes) (Schedule-2), and a schedule where we distribute a different number of tasks to different nodes based on their computation capability (Schedule-3). We present how the time taken for executing group stress analysis varies as the number of resource providers, model order, and number of members in the group vary. We considered that the data is given from all sensors to the nearby devices via bluetooth. The time taken by different devices to execute one unit task is a linear regression problem to estimate the model order. For more details on how devices are profiled and on the time taken to execute a unit task of G-causality the interested reader is refereed to [14].

Figure 4(a) shows the performance of the three scheduling approaches in terms of workload completion time. We see that centralized execution as expected takes the maximum amount of time followed by Round-Robin, whereas Schedule-3 takes the minimum amount of time. We divide our simulation into three scenarios: in Scenario-1, we assume the number of SP to be 5, number of team members to be 5 and maximum model order to be 10. In Scenario-2, we increase the maximum number of model order from 10 to 20 and in Scenario-3 we increase the number of service providers from 5 to 10 with everything else remaining the same. The result shows that time taken is very sensitive to the model order. In Scenario-4 we vary both number of service providers and order number to compare the time taken by distributing tasks under different schedules. We see that Schedule-3 takes the least amount of time. For Scenario-1 and 3, the time taken

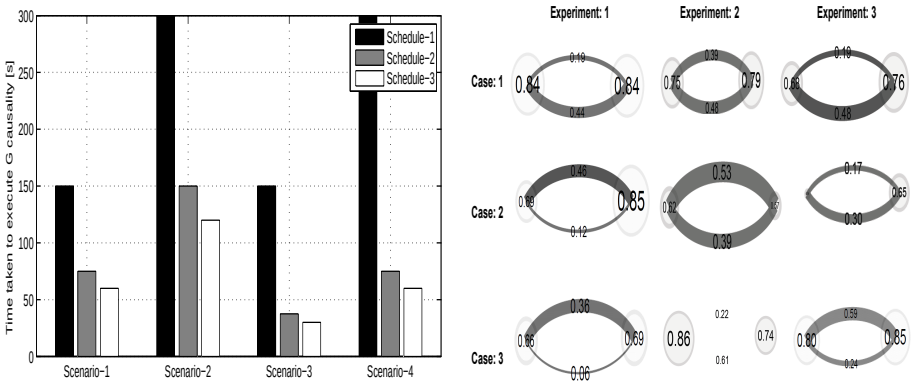

(a) (b)

Stress Propagation Test			
Phases of the Test	Type of Question	Number of Questions	Time [mins]
(Phase-1) Relaxed Phase (RX1)			2
(Phase-2) Stressed Phase (STR1) Difficulty Level: Low	Stroop Test	1	1
	Logical Questions	3	3
	Arithmetic Questions	3	3
(Phase-3) Stressed Phase (STR2) Difficulty Level: High	Memory Based	1	1
	Stroop Test	1	1
	Logical Questions	2	1
	Arithmetic Questions	2	1
(Phase-4) Relaxed Phase (RX2)			2

Figure 4: (a) Time taken for the execution of G-causality by varying time lag and number of service providers using different scheduling approaches; (b) G-causality between two team members for different cases over multiple experiments; note that the size of the node indicates stress experienced by each team member, top clockwise edge label shows magnitude of G-causality from team member A to B, and bottom edge label shows the same from team member B to A; the edge color indicates the time lag between stress data of team members to observe G-causality (white indicates lag=10, light grey indicates lag=6, dark grey indicates lag=4, and black indicates lag=1);(c) Sequence of different phases in a test to detect group stress.

of centralized execution is not affected by the number of SPs and so it remains the same. Although both Round-Robin and Schedule-3 divide the task among SPs, Round-Robin performs worse than Schedule-3 because Schedule-3 assigns tasks to SPs based on their computational capability.

Stress Propagation: We now present results for stress propagation in a group. As discussed earlier, we use G-causality to determine the extent and influence of stress from one group member to another. To quantify the mental group stress, we design our experiments to have four phases, as seen in Fig. 4(c). Phase-2 and 4 are stress inducing phases and cover questions from a wide range of topics like memory based, arithmetic, and logical questions. In our analysis a team consists of two members. One of the member of the team serves as a master and assigns tasks to the other team member. This will help us understand the propagation of stress from master to the other team member. We perform group stress detection for three different test cases: in Case-1, the first team-member serves as a master and the other team member (slave) receives instruction from the master, while in Case-2 the second member serves as the master (i.e., they switch their roles in the experiment). In Case-3 both the team members receive questions from a laptop (or a person who is not a part of the experiment). Case-3 will help us analyze the propagation of stress when each team member performs task independently. During an experiment the master assigns questions to slave, keeps track of the time, and at the end of the experiment informs the slave about his/her performance. We perform all the three cases thrice and in a random order. Each repetition of a case is termed as an experiment.

We present our results of propagation of stress using a bubble diagram as depicted in Fig. 4(b), where each member is represented by a bubble. From any node i to j the following attributes exist: *thickness* represents the magnitude of G-causality from node i to j (clockwise edge), *color* of the edge represents the model order number used to calculate the G-causality, and *size* of the node represents the average stress experienced by the person over the course of experiment. Higher the influence of G-causality, thicker is the edge, similarly higher is the stress level experienced by a team member, bigger is the bubble size. We term the left node 'A' and the right node 'B' for reference.

Now we will study the influence of G-causality between the two team members for different cases. For Case-1, node B serves as master and conducts the test for node A (slave). We see that for Case-1 in all the three experiments the influence of G-causality from node B to node A is higher than from A to B. Here, the dominant G-causality direction is from B to A and the magnitude of influence is on an average 0.25. In Case-2, for all the experiments, the influence of G-causality from node A to node B is higher than the influence from node B to A. Here, the dominant G-causality direction is from B to A and the magnitude of influence is on an average 0.12.

In Fig. 5(a) and (b) we see the average stress of team member A and B, respectively. Each subplot in Fig. 5(a) and (b) contains average stress value of a team member for a particular case over different experiments. We see that over different phases a team member exhibits different stress behavior. We begin with relaxing phase (RX1) at this point of time the stress is low and as the experiments proceed the stress level increases. We observe that in both the figures the stress level reaches a maximum before falling down again. This maximum is seen in Phase-4 (STR2) where a team member experiences the highest stress in comparison to Phase-3 (STR1). The fall in stress after STR2 is because it is followed by RX2, which is a relaxing phase.

Figure 5(c) shows the correlation between stress data of team members from each experiment over different time lags. This is done for all the three cases. We notice that

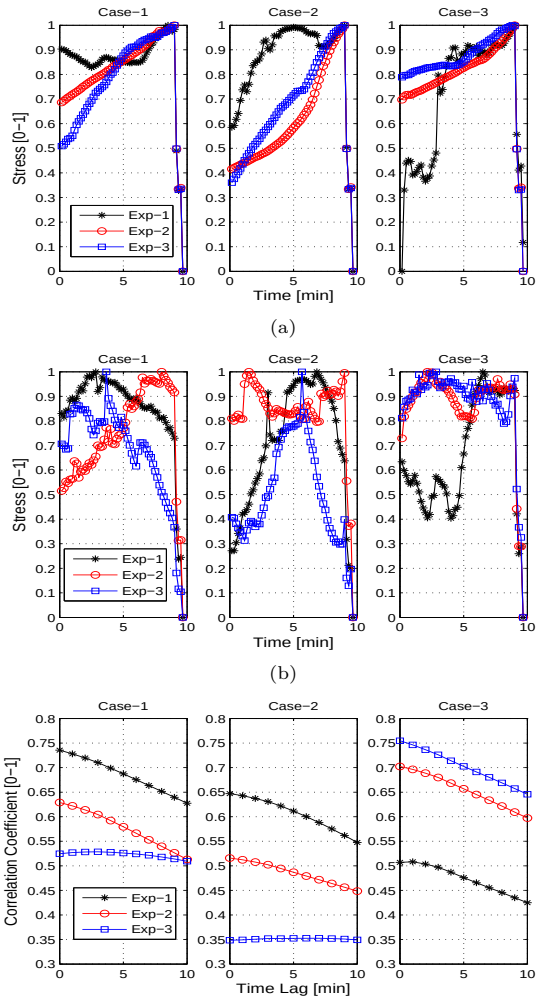

Figure 5: (a)Variation of stress over time for team-member A; (b) Variation of stress over time for team-member B; (c) Cross-correlation between team members for different time lags.

the highest correlation between stress data of different team members in Case-3 occurs when the same task is given to each team member by a PC. This is because both the team members are undergoing the experiment together and are experiencing similar level of questions and time constraint, which makes their data highly correlated as observed.

4. CONCLUSIONS

We presented real-time, in-situ stress detection via a distributed framework. In the series of experiments we saw the direction of propagation and magnitude of stress in a group. We also analyzed how this stress propagates over time. The results of this analysis helps us quantify the direction in which the stress propagates in a group. The work presented will enable taking real-time decisions and see how we can empower individuals who are in better condition (less stressed) by putting them in charge of a situation. This will help improve productivity in highly stressful situations like military operations by for example reorganizing dynamically hierarchy beyond existing ranks and roles.

Acknowledgements

This work was supported by the DARPA Young Faculty Award (YFA) grant no. 11038087. The authors are in debt with Abolfazl Hajisami and Shilpa Shivalingaiah for their help with the experiments.

5. REFERENCES

[1] H. Akaike. A new Look at the Statistical Model Identification. *IEEE Transactions on Automatic Control*, 19(6):716–723, 1974.

[2] A. Barrett et al. Granger Causality Analysis of Steady-state Electroencephalographic Signals during Propofol-induced Anaesthesia. *PloS one*, 7(1):29–72, 2012.

[3] S. Bruce, H. Conaglen, and J. Conaglen. Burnout in physicians: A Case for Peer-support. *Internal Medicine Journal*, 35(5):272–278, 2005.

[4] A. De Santos, C. Sanchez-Avila, J. Guerra-Casanova, and G. Bailador-Del Pozo. Real-time Stress Detection by means of Physiological Signals. In *Recent Application in Biometrics*. InTech, 2011.

[5] A. de Santos Sierra, C. Avila, G. Bailador del Pozo, and J. Guerra Casanova. Stress Detection by Means of Stress Physiological Template. In *Proc. of Nature and Biologically Inspired Computing (NaBIC)*, pages 131–136, 2011.

[6] J. Geweke. Measurement of linear dependence and feedback between multiple time series. *Journal of the American Statistical Association*, 77(378):304–313, 1982.

[7] J. Jin, X. Wang, S. Li, and Y. Wu. A Novel Heart Rate Detection Algorithm in Ballistocardiogram Based on Wavelet Transform. In *Second International Workshop on Knowledge Discovery and Data Mining*, Moscow, January 2009.

[8] C. L. Lisetti and F. Nasoz. Using Noninvasive Wearable Computers to Recognize Human Emotions from Physiological Signals. *EURASIP Journal on Applied Signal Processing*, 2004:1672–1687, 2004.

[9] M. B. Schippers, R. Renken, and C. Keysers. The Effect of intra-and inter-subject Variability of Hemodynamic Responses on Group Level Granger Causality Analyses. *NeuroImage*, 57(1):22–36, 2011.

[10] G. Schwarz. Estimating the Dimension of a Model. *The Annals of Statistics*, 6(2):461–464, 1978.

[11] A. K. Seth. A MATLAB Toolbox for Granger Causal Connectivity Analysis. *Journal of Neuroscience Methods*, 186(2):22–26, 2010.

[12] L. A. Simpson and L. Grant. Sources and Magnitude of Job Stress among Physicians. *Journal of Behavioral Medicine*, 14(1):27–42, 1991.

[13] F.-T. Sun, C. Kuo, H.-T. Cheng, S. Buthpitiya, P. Collins, and M. L. Griss. Activity-Aware Mental Stress Detection Using Physiological Sensors. In *Proc. of Intl. Conf. on Mobile Computing, Application, and Services (MobiCASE)*, Santa Clara, CA, October 2010.

[14] H. Viswanathan, E. K. Lee, and D. Pompili. Enabling Real-time In-Situ Processing of Ubiquitous Mobile-Application Workflows. In *Proc. of IEEE International Conference on Mobile Ad-hoc and Sensor Systems (MASS)*, Hangzhou, China, October 2013.

[15] H. Viswanathan, E. K. Lee, I. Rodero, and D. Pompili. An Autonomic Resource Provisioning Framework for Mobile Computing Grids. In *Proc. of IEEE International Conference on Autonomic Computing (ICAC)*, San Jose, CA, September 2012.

[16] A. D. Waterman, J. Garbutt, E. Hazel, W. C. Dunagan, W. Levinson, V. J. Fraser, and T. H. Gallagher. The Emotional Impact of Medical Errors on Practicing Physicians in the United States and Canada. *Joint Commission Journal on Quality and Patient Safety*, 33(8):467–476, 2007.